Vol 13 No 7, July 2004
1009-1963/2004/13(07)/1082-09

Chinese Physics

© 2004 Chin. Phys. Soc.
and IOP Publishing Ltd

Calculation of the surface energy of fcc metals with modified embedded-atom method*

Zhang Jian-Min(张建民)[a)†], Ma Fei(马 飞)[a)], and Xu Ke-Wei(徐可为)[b)]

[a)] *College of Physics and Information Technology, Shaanxi Normal University, Xi'an* 710062, *China*

[b)] *State Key Laboratory for Mechanical Behaviour of Materials, Xi'an Jiaotong University, Xi'an* 710049, *China*

(Received 10 June 2003; revised manuscript received 19 December 2003)

The surface energies for 38 surfaces of fcc metals Cu, Ag, Au, Ni, Pd, Pt, Al, Pb, Rh and Ir have been calculated by using the modified embedded-atom method. The results show that, for Cu, Ag, Ni, Al, Pb and Ir, the average values of the surface energies are very close to the polycrystalline experimental data. For all fcc metals, as predicted, the close-packed (111) surface has the lowest surface energy. The surface energies for the other surfaces increase linearly with increasing angle between the surfaces (hkl) and (111). This can be used to estimate the relative values of the surface energy.

Keywords: fcc metals, surface energy, calculation, modified embedded-atom method
PACC: 6150C, 6810C, 6820, 7110

1. Introduction

Thin metal films are used extensively in decorative, protective, electronic, magnetic and optical devices and systems. In all of these applications, the physical, chemical and mechanical properties of the films are affected by microstructural attributes such as grain size, grain size distribution, defect density, and texture. Film texture is of particular interest owing to the anisotropic variations observed in the films. For example, the value of the elastic modulus of Cu in the $< 111 >$ direction is 2.9 times higher than the value in the $< 100 >$ direction.[1] Reaction rates for oxide [2] and silicide [3] formation on Cu are faster along the (100) surface than along the (111) surface. For Cu, Al and Ag films, several experimental results showed that both the residual compressive stress and resistivity increase with increasing (100) texture; in contrast, they decrease with increasing (111) texture.[4−8] Based on the elastic theory,[9] we have made a calculation of the stresses in the plane of the film for different-oriented grains in a polycrystalline film grown from one of the face-centred cubic (fcc) metals, such as Cu, Al, Ag, Au, Ni, Pb and Th. The relationship between texture and stress mentioned above has been explained satisfactorily by the calculated results.[10]

The preferred orientations or textures of the films, in turn, are strongly affected by the conditions under which the films are formed and can be modified through abnormal grain growth during post-processing such as annealing. Ohmi *et al* found that, under relatively low-energy ion bombardment conditions, (100)- or (111)-oriented Cu films could be grown epitaxially on (100) Si or (111) Si surfaces, respectively. On the other hand, completely (111)-oriented films were obtained either on (100) Si, (111) Si, or SiO_2 surfaces when large ion-bombardment energies were employed. They also found that (111)-oriented films thus created on SiO_2 were metastable and easily transformed by thermal annealing into completely (100)-oriented films with large grains of about 100μm.[11,12] For Cu, Al and Ag films, (111), (100) and (110) fibre texture components for evaporated,[3,13−17] sputtered,[17,18] partially ionized beam deposited,[17,19] electroplated [13,17] and electroless plated [20] samples have also been reported. In a previous paper,[21] x-ray diffraction patterns showed that, after annealing at 300°C for 2h, the free-standing Cu and Ag films exhibited a slight increase in (111) texture. In contrast, both Cu and Ag films attached to a Si substrate showed an increase

*Project supported by the National Natural Science Foundation of China (Grant Nos 50271038 and 59931010).
†Author to whom correspondence should be addressed. E-mail: jianm_zhang@yahoo.com

in (100) and (110) texture. The former results from minimization of surface energy. Because in the films with a fcc structure, the close-packed (111) plane is predicted to have the lowest surface energy and for a free-standing film there are two free surfaces and no effects of film-substrate interface energy and thermal strain energy. The latter is driven by minimization of strain energy.[22]

Different from the bulk materials, thin films have a relatively large surface and interface. The anisotropy of the surface and interface energies can supply an additional driving force for abnormal grain growth and for texture formation or change in a thin polycrystalline film on a substrate.[23] The behaviour consistent with surface-energy-driven secondary grain growth (SEDSGG) has been observed in Au,[24] alloyed Al,[25,26] Si [27,28] and Ge [29] films. Lee [30] suggested that the texture of the film changed from the orientation that placed the lowest surface energy plane parallel to the substrate surface under the conditions of low atomic or ionic concentration adjacent to the substrate, to the orientation that placed the higher surface energy planes parallel to the substrate surface with increasing atomic or ionic concentration adjacent to the substrate.

In this paper, the surface energies of various surfaces have been calculated for fcc metals Cu, Ag, Au, Ni, Pd, Pt, Al, Pb, Rh and Ir by using the modified embedded-atom method (MEAM),[31,32] which is an extension of the initial embedded-atom method (EAM) [33,34] by including directional bonding. The EAM is based on density-functional theory [35,36] and has been used quite successfully in predicting numerous properties of metals and alloys: for example, hydrogen embrittlement,[33] defects,[34,37,38] surface structure [33,37] and reconstruction,[39,40] segregation [41] and phase stability [42] in alloys, bulk and surface phonons,[43] and liquids.[44]

2. Modified embedded-atom method

In the EAM, the total energy E of a system of atoms is given by the expression [33,34]

$$E = \sum_i \left[F_i\left(\overline{\rho}_i\right) + \frac{1}{2}\sum_{j(\neq i)} \phi_{ij}\left(R_{ij}\right)\right], \qquad (1)$$

where the embedding function F_i is the energy to embed an atom i into the background electron density at site i, $\overline{\rho}_i$; and ϕ_{ij} is a pair interaction between atoms i and j separated by a distance R_{ij}. $\overline{\rho}_i$ is given by a linear supposition of spherically averaged atomic electron densities.

The term in parentheses in Eq.(1) denotes the contribution to the total energy from the ith atom

$$E_i = F_i\left(\overline{\rho}_i / Z_i\right) + \frac{1}{2}\sum_{j(\neq i)} \phi_{ij}\left(R_{ij}\right). \qquad (2)$$

For simplification, Baskes [45] has normalized the background electron density by the number of nearest neighbours Z_i defined as the reference structure of a type-i atom. The reference structure is usually the equilibrium crystal structure of type-i atoms.

In the case of homogeneous monatomic solid with interactions limited to the first neighbours only, the energy of each atom in this reference structure is shown simply as [45]

$$E_i^{\mathrm{u}}(R) = F_i\left(\bar{\rho}_i^0(R)/Z_i\right) + \frac{Z_i}{2}\phi_{ii}(R), \qquad (3)$$

where $\bar{\rho}_i^0(R)$ is the background electron density for the reference structure of atom i and R is the nearest-neighbour distance. Assuming that $E_i^{\mathrm{u}}(R)$ is known, the pair interaction for type-i atoms is then shown as

$$\phi_{ii}(R) = \frac{2}{Z_i}\left\{E_i^{\mathrm{u}}(R) - F_i\left(\bar{\rho}_i^0(R)/Z_i\right)\right\}. \qquad (4)$$

Using this definition of the pair interaction, Baskes has given the energy contribution E_i for any configuration of atoms and the unrelaxed surface energy $E_{(x)}^f$:

$$E_i = \frac{1}{Z_i}\sum_{j(\neq i)} E_i^{\mathrm{u}}\left(R_{ij}\right) + \left[F_i\left(\overline{\rho}_i/Z_i\right) - \frac{1}{Z_i}\sum_{j(\neq i)} F\left(\overline{\rho}_i^0\left(R_{ij}\right)/Z_i\right)\right], \qquad (5)$$

$$E_{(x)}^f = \sum\left[E_i^0\frac{Z_i - Z_d}{Z_i} + F_i\left(\overline{\rho}_i^x/Z_i\right) - \frac{Z_d}{Z_i}F_i\left(\overline{\rho}_i^0/Z_i\right)\right]/A_{(x)}, \qquad (6)$$

where E_i^0 is the negative of the minimum energy of the reference lattice (sublimation energy), $\overline{\rho}_i^x$ is the background electron density at site i, a nearest neighbour to the surface, $A_{(x)}$ is the area per atom on the surface, and Z_d is the number of the nearest neighbours to site i. Since for some surfaces there is more than one type of site i, a sum over the different environments (planes) in Eq.(6) is indicated.

Baskes has also generalized the original background electron densities of EAM (Eq.(7)) by defining a series of correction electron densities that explicitly

depend upon the relative positions of neighbours of atom i (Eqs.(8)–(10)):

$$\rho_i^{(0)} = \sum_{j(\neq i)} \rho_j^{a(0)}(R_{ij}), \tag{7}$$

$$\left(\rho_i^{(1)}\right)^2 = \sum_{\alpha} \left[\sum_{j(\neq i)} x_{ij}^{\alpha} \rho_j^{a(1)}\left(R_{ij}\right)\right]^2, \tag{8}$$

$$\left(\rho_i^{(2)}\right)^2 = \sum_{\alpha,\beta} \left[\sum_{j(\neq i)} x_{ij}^{\alpha} x_{ij}^{\beta} \rho_j^{a(2)}\left(R_{ij}\right)\right]^2 - \frac{1}{3}\left[\sum_{j(\neq i)} \rho_j^{a(2)}\left(R_{ij}\right)\right]^2, \tag{9}$$

$$\left(\rho_i^{(3)}\right)^2 = \sum_{\alpha,\beta,\gamma} \left[\sum_{j(\neq i)} x_{ij}^{\alpha} x_{ij}^{\beta} x_{ij}^{\gamma} \rho_j^{a(3)}\left(R_{ij}\right)\right]^2, \tag{10}$$

where $\rho_j^{a(l)}(R_{ij})$ (l=0, 1, 2, 3) represents the atomic electron density of a type-j atom at a distance of R_{ij} from site i. $x_{ij}^{\alpha} = R_{ij}^{\alpha}/R_{ij}$, R_{ij}^{α} is the α component of distance vector between atoms j and i. The total background electron density is expressed by taking a weighted sum of the squares of the partial background densities

$$(\bar{\rho}_i)^2 = \sum_{l=0}^{3} t_i^{(l)} \left(\rho_i^{(l)}\right)^2, \tag{11}$$

with $t_i^{(l)}$ (l=0, 1, 2, 3) as the weighting factors as well as $t_i^{(0)} = 1$. Using Eq.(11), the background electron densities for the reference structure $\bar{\rho}_i^0$ used in Eqs.(3)–(6) and the surface background electron density $\bar{\rho}_i^x$ in Eq.(6) can be written as

$$\left(\bar{\rho}_i^0\right)^2 = \sum_{l=0}^{3} t_i^{(l)} s_i^{(l),0} \left(\rho_i^{a(l)}\left(R\right)\right)^2, \tag{12}$$

$$(\bar{\rho}_i^x)^2 = \sum_{l=0}^{3} t_i^{(l)} s_i^{(l),x} \left(\rho_i^{a(l)}(R)\right)^2. \tag{13}$$

The factors $s_i^{(l),0}$ and $s_i^{(l),x}$ (l=0, 1, 2, 3) depend only on the geometry and will be determined in detail in the next section.

3. Determination of geometric factors

For an unrelaxed monatomic solid, the atomic density factors $\rho_j^{a(l)}(R_{ij})$ (l=0, 1, 2, 3) could be taken out of the sum due to the equality in the nearest-neighbour distances ($R_{ij} = R$). Inserting Eqs.(7)–(10) into Eq.(11) and comparing with Eq.(13), we can obtain

$$s_i^{(0),x} = \left(Z_d\right)^2, \tag{14}$$

$$s_i^{(1),x} = \sum_{\alpha} \left[\sum_{j(\neq i)} x_{ij}^{\alpha}\right]^2, \tag{15}$$

$$s_i^{(2),x} = \sum_{\alpha,\beta} \left[\sum_{j(\neq i)} x_{ij}^{\alpha} x_{ij}^{\beta}\right]^2 - \frac{1}{3}\left(Z_d\right)^2, \tag{16}$$

$$s_i^{(3),x} = \sum_{\alpha,\beta,\gamma} \left[\sum_{j(\neq i)} x_{ij}^{\alpha} x_{ij}^{\beta} x_{ij}^{\gamma}\right]^2. \tag{17}$$

In a coordinate system with x, y and z as the orthogonal axes, Eqs.(15)–(17) can be expressed distinctly as

$$s_i^{(1),x} = \left[\sum_{j(\neq i)} x_{ij}^{x}\right]^2 + \left[\sum_{j(\neq i)} x_{ij}^{y}\right]^2 + \left[\sum_{j(\neq i)} x_{ij}^{z}\right]^2, \tag{18}$$

$$s_i^{(2),x} = \left[\sum_{j(\neq i)} \left(x_{ij}^{x}\right)^2\right]^2 + \left[\sum_{j(\neq i)} \left(x_{ij}^{y}\right)^2\right]^2 + \left[\sum_{j(\neq i)} \left(x_{ij}^{z}\right)^2\right]^2 + 2\left\{\left[\sum_{j(\neq i)} x_{ij}^{x} x_{ij}^{y}\right]^2 + \left[\sum_{j(\neq i)} x_{ij}^{x} x_{ij}^{z}\right]^2 + \left[\sum_{j(\neq i)} x_{ij}^{y} x_{ij}^{z}\right]^2\right\} - \frac{1}{3}\left(Z_d\right)^2, \tag{19}$$

$$s_i^{(3),x} = \left[\sum_{j(\neq i)} \left(x_{ij}^{x}\right)^3\right]^2 + \left[\sum_{j(\neq i)} \left(x_{ij}^{y}\right)^3\right]^2 + \left[\sum_{j(\neq i)} \left(x_{ij}^{z}\right)^3\right]^2 + 6 \times \left\{\left[\sum_{j(\neq i)} x_{ij}^{x} x_{ij}^{y} x_{ij}^{z}\right]^2\right\} + 3\left\{\left[\sum_{j(\neq i)} \left(x_{ij}^{x}\right)^2 x_{ij}^{y}\right]^2 + \left[\sum_{j(\neq i)} \left(x_{ij}^{x}\right)^2 x_{ij}^{z}\right]^2 + \left[\sum_{j(\neq i)} x_{ij}^{x} \left(x_{ij}^{y}\right)^2\right]^2 + \left[\sum_{j(\neq i)} x_{ij}^{x} \left(x_{ij}^{z}\right)^2\right]^2 + \left[\sum_{j(\neq i)} \left(x_{ij}^{y}\right)^2 x_{ij}^{z}\right]^2 + \left[\sum_{j(\neq i)} x_{ij}^{y} \left(x_{ij}^{z}\right)^2\right]^2\right\}. \tag{20}$$

In the present study, a computer program written in C language has been developed to calculate the geometric factors $S_i^{(1),x}$, the number of the nearest neighbours to type-i site, Z_d, and area factors $A_{(x)}$ for a fcc lattice. The calculated results are listed in Table 1.

Table 1. Parameters for the perfect lattice ($x = 0$) and surfaces ($x = (hkl)$) of a fcc lattice: the number of the nearest neighbours to type-i site Z_d, values of the geometric factors $S_i^{(1),x}$ (l=0, 1, 2, 3), the number of types corresponding to identical Z_d and $S_i^{(1),x}$ values N, and area factors $A_{(x)}$. The lattice constant is a_i^0.

(hkl)	Z_d	$S_i^{(0),x}$	$S_i^{(1),x}$	$S_i^{(2),x}$	$S_i^{(3),x}$	N	$A_{(x)}/(a_i^0)^2$
Perfect lattice	12	144	0	0.00000	0.00	1	−−
(100)	8	64	8	0.66667	5.00	1	0.50000
(110)	7	49	9	0.66667	6.00	1	0.70711
	11	121	1	0.66667	1.00	1	
(111)	9	81	6	1.50000	3.75	1	0.43301
(210)	6	36	10	0.00000	7.00	1	1.11803
	9	91	5	1.00000	3.50	1	
	11	121	1	0.66667	1.00	1	
(211)	7	49	9	0.66667	6.00	1	1.22475
	9	81	6	1.50000	3.75	1	
	10	100	3	1.16667	2.25	1	
(221)	7	49	9	0.66667	6.00	1	1.50000
	9	81	6	1.50000	3.75	2	
	11	121	1	0.66667	1.00	1	
(310)	6	36	10	0.00000	7.00	1	1.58114
	8	64	8	0.66667	5.00	1	
	9	81	5	1.00000	3.50	1	
	11	121	1	0.66667	1.00	1	
(311)	7	49	9	0.66667	6.00	1	0.82916
	10	100	3	1.16667	2.25	1	
(320)	6	36	10	0.00000	7.00	1	1.80278
	11	121	1	0.66667	1.00	2	
	9	81	5	1.00000	3.50	1	
	7	49	9	0.66667	6.00	1	
(321)	6	36	10	0.00000	7.00	1	1.87083
	9	81	6	1.50000	3.75	1	
	11	121	1	0.66667	1.00	1	
	8	64	7	1.16667	4.75	1	
	10	100	3	1.16667	2.25	1	
(322)	7	49	9	0.66667	6.00	1	2.06155
	10	100	3	1.16667	2.25	1	
	9	81	6	1.50000	3.75	3	
(331)	7	49	9	0.66667	6.00	1	1.08973
	9	91	6	1.50000	3.75	1	
	11	121	1	0.66667	1.00	1	
(332)	7	49	9	0.66667	6.00	1	2.34520
	11	121	1	0.66667	1.00	1	
	9	81	6	1.50000	3.75	4	
(410)	6	36	10	0.00000	7.00	1	2.06156
	11	121	1	0.66667	1.00	1	
	8	64	8	0.66667	5.00	2	
	9	81	5	1.00000	3.50	1	
(411)	7	49	9	0.66667	6.00	2	2.12132
	10	100	3	1.16667	2.25	2	
	8	64	8	0.66667	5.00	1	

Table 1. (*Continued*)

(421)	6	36	10	0.00000	7.00	1	2.29129
	8	64	7	1.16667	4.75	1	
	10	100	3	1.16667	2.25	2	
	7	49	9	0.66667	6.00	1	
	11	121	1	0.66667	1.00	1	
(430)	6	36	10	0.00000	7.00	1	2.50000
	11	121	1	0.66667	1.00	3	
	7	49	9	0.66667	6.00	2	
	9	81	5	1.00000	3.50	1	
(431)	6	36	10	0.00000	7.00	1	2.54951
	8	64	7	1.16667	4.75	1	
	10	100	3	1.16667	2.25	1	
	11	121	1	0.66667	1.00	2	
	7	49	9	0.66667	6.00	1	
	9	81	6	1.50000	3.75	1	
(433)	7	49	9	0.66667	6.00	1	2.91548
	10	100	3	1.16667	2.25	1	
	9	81	6	1.50000	3.75	5	
(441)	7	49	9	0.66667	6.00	3	
	11	121	1	0.66667	1.00	3	2.87228
	9	81	6	1.50000	3.75	2	
(443)	7	49	9	0.66667	6.00	1	3.20156
	11	121	1	0.66667	1.00	1	
	9	81	6	1.50000	3.75	6	
(510)	6	36	10	0.00000	7.00	1	2.54951
	11	121	1	0.66667	1.00	1	
	8	64	8	0.66667	5.00	3	
	9	81	5	1.00000	3.50	1	
(511)	7	49	9	0.66667	6.00	1	1.29904
	10	100	3	1.16667	2.25	1	
	8	64	8	0.66667	5.00	1	
(520)	6	36	10	0.00000	7.00	2	2.69258
	9	81	5	1.00000	3.50	2	
	8	64	8	0.66667	5.00	1	
	11	121	1	0.66667	1.00	2	
(521)	6	36	10	0.00000	7.00	1	2.73861
	7	49	9	0.66667	1.00	1	
	10	100	3	1.16667	2.25	2	
	11	121	1	0.66667	1.00	1	
	9	81	5	1.00000	3.50	1	
(522)	7	49	9	0.66667	6.00	3	2.87228
	10	100	3	1.16667	2.25	3	
	9	81	6	1.50000	3.75	1	
(530)	6	36	10	0.00000	7.00	2	2.91548
	11	121	1	0.66667	1.00	3	
	7	49	9	0.66667	6.00	1	
	9	81	5	1.00000	3.50	2	

Table 1. (*Continued*)

(531)	6	36	10	0.00000	7.00	1	1.47902
	8	64	7	1.16667	4.75	1	
	10	100	3	1.16667	2.25	1	
	11	121	1	0.66667	1.00	1	
(532)	6	36	10	0.00000	7.00	1	3.08221
	9	81	5	1.50000	3.75	2	
	7	49	9	0.66667	6.00	1	
	10	100	3	1.16667	2.25	2	
	8	64	7	1.16667	4.75	1	
	11	121	1	0.66667	1.00	1	
(533)	7	49	9	0.66667	6.00	1	1.63936
	10	100	3	1.16667	2.25	1	
	9	81	6	1.50000	3.75	2	
(540)	6	36	10	0.00000	7.00	1	3.20156
	11	121	1	0.66667	1.00	4	
	7	49	9	0.66667	6.00	3	
	9	81	5	1.00000	3.50	1	
(541)	6	36	10	0.00000	7.00	1	3.24037
	7	49	9	0.66667	6.00	2	
	11	121	1	0.66667	1.00	3	
	9	81	6	1.50000	3.75	1	
	10	100	3	1.16667	2.25	1	
	8	64	7	1.16667	4.75	1	
(542)	6	36	10	0.00000	7.00	2	3.35410
	9	81	5	1.50000	3.75	4	
	11	121	1	0.66667	1.00	3	
	7	49	9	0.66667	6.00	1	
(544)	7	49	9	0.66667	6.00	1	3.77492
	10	100	3	1.16667	2.25	1	
	9	81	6	1.50000	3.75	7	
(551)	7	49	9	0.66667	6.00	2	1.78536
	11	121	1	0.66667	1.00	2	
	9	81	6	1.50000	3.75	1	
(552)	7	49	9	0.66667	6.00	3	3.67424
	11	121	1	0.66667	1.00	3	
	9	81	6	1.50000	3.75	4	
(553)	7	49	9	0.66667	6.00	1	1.92029
	11	121	1	0.66667	1.00	1	
	9	81	6	1.50000	3.75	3	
(554)	7	49	9	0.66667	6.00	1	4.06202
	11	121	1	0.66667	1.00	1	
	9	81	6	1.50000	3.75	8	

4. Calculation of surface energy for fcc metals

To calculate surface energy with Eq.(6), suitable forms of embedding function $F_i(\rho)$ and atomic electron density $\rho_i^{a(l)}(R)$ should be selected. We take the following form given by Baskes *et al*[31,32,45]

$$F_i(\rho) = A_i E_i^0 \rho \ln \rho, \tag{21}$$

$$\rho_i^{a(l)}(R) = \mathrm{e}^{-b}, \tag{22}$$

$$b = \beta_i^{(l)} \left(\frac{R}{R_i^0} - 1 \right), \tag{23}$$

where A_i and $\beta_i^{(l)}$ are parameters to be determined. E_i^0 is the sublimation energy. R_i^0 is the equilibrium nearest-neighbour distance. For unrelaxed surfaces,

$R_i^0 = R$. Eq.(22) becomes

$$\rho_i^{a(l)}(R) = 1. \tag{24}$$

So Eqs.(12) and (13) are simplified as

$$\bar{\rho}_i^0 = \left(\sum_{l=0}^{3} t_i^{(l)} s_i^{(l),0}\right)^{\frac{1}{2}}, \tag{25}$$

$$\bar{\rho}_i^x = \left(\sum_{l=0}^{3} t_i^{(l)} s_i^{(l),x}\right)^{\frac{1}{2}}. \tag{26}$$

The other parameters needed in this calculation are taken from Ref.[45]. For convenience, they are listed in Table 2.

Table 2. Parameters for the MEAM. Values listed are the sublimation energy E_i^0 (eV), the equilibrium nearest-neighbour distance R_i^0 (nm), the scaling factor for the embedding energy A_i, and the weighting factors for the atomic electron densities $t_i^{(l)}$ (l=0, 1, 2, 3).[45]

Metals	E_i^0/eV	R_i^0/nm	A_i	$t_i^{(0)}$	$t_i^{(1)}$	$t_i^{(2)}$	$t_i^{(3)}$
Cu	3.54	0.256	1.07	1	3.14	2.49	2.95
Ag	2.85	0.288	1.06	1	5.54	2.45	1.29
Au	3.93	0.288	1.04	1	1.59	1.51	2.61
Ni	4.45	0.249	1.10	1	3.57	1.60	3.70
Pd	3.91	0.275	1.01	1	2.34	1.38	4.48
Pt	5.77	0.277	1.04	1	2.73	−1.38	3.29
Al	3.58	0.286	1.07	1	−1.78	−2.21	8.01
Pb	2.04	0.350	1.01	1	2.74	3.06	1.20
Rh	5.75	0.269	1.05	1	2.99	4.61	4.80
Ir	6.93	0.272	1.05	1	1.50	8.10	4.80

Inserting the parameters listed in Table 1 and Table 2 into Eqs.(25), (26), (21), and then into Eq.(6), we can obtain the unrelaxed surface energies for various surfaces of the fcc metals Cu, Ag, Au, Ni, Pd, Pt, Al, Pb, Rh and Ir. The results are listed in Table 3 together with the angles $\theta_{(hkl)}$ (in degree) included between the corresponding planes and close-packed (111) plane (column 2). The angle $\theta_{(hkl)}$ included between planes (hkl) and (111) is calculated with Eq.(27)

$$\cos\theta_{(hkl)} = \frac{h+k+l}{\sqrt{3\times(h^2+k^2+l^2)}}. \tag{27}$$

To compare with the experimental data for polycrystalline samples,[45] the average energy of various surfaces of each metal is also given in Table 3.

Table 3. Calculated values of the surface energy/(10^{-7}J/cm^2) for various surfaces of the fcc metals Cu, Ag, Au, Ni, Pd, Pt, Al, Pb, Rh and Ir, the average values of various surfaces of each metal (row 40) and angles $\theta_{(hkl)}$/(°) included between plane (hkl) and plane (111) (column 2). The experimental polycrystalline average values (last row) are accurate at least to about 10% and in a number of cases, indicated by an asterisk, have been crudely extrapolated from the melt temperature to 0K.[45]

(hkl)	$\theta_{(hkl)}$	Cu	Ag	Au	Ni	Pd	Pt	Al	Pb	Rh	Ir
(100)	54.74	1650.56	1275.21	1082.81	2433.53	1660.50	2167.91	900.36	424.11	2896.29	2895.10
(110)	35.26	1640.89	1225.82	1114.44	2382.53	1671.21	2131.73	972.32	431.03	2914.50	3046.76
(111)	0.00	1408.62	1091.16	885.79	2035.49	1382.40	1655.98	619.96	366.42	2593.08	2823.75
(210)	39.23	1712.98	1269.34	1182.30	2488.98	1757.55	2269.26	1068.20	451.40	3018.21	3128.80
(211)	19.47	1611.50	1222.17	1061.00	2335.23	1616.62	2011.59	853.47	421.60	2905.14	3090.19
(221)	15.79	1521.18	1164.49	999.65	2204.96	1514.97	1897.02	791.06	404.97	2716.76	2867.47
(310)	43.09	1733.21	1300.82	1178.43	2529.52	1767.87	2290.16	1040.05	453.30	3050.08	3127.91
(311)	29.50	1644.73	1235.44	1104.62	2386.40	1666.00	2106.53	936.90	431.40	2937.02	3072.65
(320)	36.81	1705.95	1268.02	1170.35	2478.11	1745.49	2243.47	1043.84	449.01	3014.97	3135.44
(321)	22.21	1656.59	1240.74	1114.07	2397.73	1677.55	2108.23	941.05	435.84	2967.71	3147.71
(322)	11.42	1549.09	1184.44	1002.43	2242.39	1541.12	1890.69	767.46	404.39	2815.19	3022.02
(331)	22.00	1624.46	1228.99	1075.12	2354.79	1633.72	2041.25	877.26	425.28	2921.53	3099.01
(332)	10.02	1535.06	1175.45	990.20	2221.63	1524.83	1865.73	751.02	400.57	2793.82	3004.06

Table 3. (*Continued*)

(410)	45.56	1729.63	1306.96	1166.43	2530.27	1758.62	2282.27	1016.05	450.53	3041.76	3101.16
(411)	35.26	1674.79	1266.36	1118.75	2439.12	1693.75	2157.73	944.63	437.21	2978.63	3097.87
(421)	28.13	1681.59	1253.93	1141.97	2436.65	1711.35	2170.72	990.24	442.73	2995.92	3154.63
(430)	36.07	1482.94	1100.65	1021.87	2154.48	1515.82	1958.47	915.87	390.65	2609.31	2907.00
(431)	25.07	1584.18	1190.06	1073.72	2301.03	1601.65	2053.80	921.35	418.61	2795.06	2911.05
(433)	8.05	1513.79	1161.64	971.93	2190.22	1500.36	1828.80	726.83	394.79	2760.87	2975.65
(441)	25.24	1636.58	1234.31	1090.14	2373.32	1651.07	2073.67	905.02	428.81	2934.32	3101.55
(443)	7.33	1505.48	1156.19	964.94	2177.97	1490.90	1814.61	717.83	392.54	2747.93	2964.33
(510)	47.21	1722.30	1306.91	1155.55	2523.25	1747.69	2270.62	998.16	447.48	3027.60	3075.40
(511)	38.94	1685.11	1279.39	1121.84	2459.87	1702.51	2179.00	944.56	438.60	2989.44	3086.56
(520)	41.37	1729.05	1290.93	1182.92	2518.88	1767.91	2287.09	1054.28	453.62	3044.31	3135.94
(521)	32.51	1695.25	1266.30	1151.55	2461.16	1726.33	2201.99	1003.41	445.51	3010.63	3148.36
(522)	25.24	1636.73	1234.41	1090.17	2373.53	1651.20	2073.95	904.84	428.84	2934.44	3101.62
(530)	37.62	1711.77	1270.85	1177.08	2486.81	1753.31	2257.46	1055.09	450.75	3021.73	3138.63
(531)	28.56	1683.05	1249.98	1149.87	2437.00	1717.23	2181.91	1008.84	444.03	2994.73	3154.90
(532)	20.51	1645.85	1238.74	1097.81	2383.29	1660.61	2078.97	910.33	432.07	2955.71	3138.51
(533)	14.42	1575.98	1201.27	1026.62	2282.25	1572.89	1940.22	801.36	411.76	2855.29	3054.47
(540)	35.76	1685.43	1255.49	1151.30	2447.83	1721.09	2204.92	1017.28	443.23	2985.12	3111.37
(541)	27.02	1672.57	1251.33	1129.59	2424.15	1697.91	2147.55	967.67	439.75	2985.40	3147.05
(542)	18.79	1900.23	1196.98	1064.55	2302.50	1603.01	2012.62	883.79	419.49	2847.13	3020.41
(544)	6.21	1492.29	1147.49	953.86	2158.53	1475.91	1792.33	703.57	388.96	2727.18	2945.97
(551)	27.22	1641.41	1235.63	1097.60	2380.91	1659.07	2090.21	920.55	430.29	2937.52	3098.23
(552)	19.47	1611.38	1222.09	1060.98	2335.07	1616.52	2011.37	853.61	421.58	2905.04	3090.13
(553)	12.27	1557.10	1189.51	1009.58	2254.25	1550.53	1905.17	777.41	406.58	2827.32	3032.06
(554)	5.77	1486.88	1143.90	949.39	2150.57	1469.80	1783.27	697.94	387.50	2718.67	2938.40
Average values		1629.90	1224.56	1081.09	2354.58	1636.23	2064.17	900.09	424.87	2899.35	3049.79
Experimental values		1770	1320	1540	2240	2000*	2500*	1000	600*	2600*	3000*

We can see that, from the last two rows of Table 3, for Cu, Ag, Ni, Al, Pb and Ir, the average surface energies are very close to the polycrystalline experimental data. For Ni, Rh and Ir, the average surface energies are higher than the experimental values. For Cu, Ag, Au, Pd, Pt, Al, and Pb, the average surface energies are lower than the experimental values.

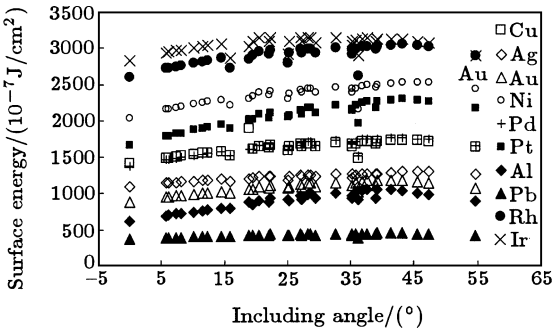


Fig.1. Variation of surface energy with the angle included between planes (*hkl*) and (111).

Figure 1 shows the variations of surface energy with the angle included between planes (*hkl*) and (111). We see that, for all the fcc metals considered here, the lowest surface energy, as predicted, corresponds to the close-packed (111) plane. The surface energies corresponding to the other planes increase linearly with increasing angle included between planes (*hkl*) and (111). So a deviation of a crystal plane from (111) plane can be used to estimate the relative values of the surface energy.

5. Conclusions

In addition to grain boundary energy as in the case of the bulk materials, the anisotropy of surface and/or interface energies can supply an additional driving force for preferred orientation growth or texture in a thin polycrystalline film. The surface energies for 38 surfaces of fcc metals Cu, Ag, Au, Ni, Pd, Pt, Al, Pb, Rh and Ir have been calculated by using the modified embedded-atom method. The results show that, for Cu, Ag, Ni, Al, Pb and Ir, the average surface energies are very close to the poly-

crystalline experimental data. For all fcc metals considered here, the lowest surface energy corresponds to the close-packed (111) plane as predicted from the fcc lattice. So from surface energy minimization, the (111) texture should be favourable in a fcc film. The surface energies corresponding to the other planes increase linearly with increasing angle included between planes (hkl) and (111). This can be used to estimate the relative values of surface energy for surfaces in different orientations.

References

[1] Hertzberg R W 1989 *Deformation and Fracture Mechanics of Engineering Materials* (New York: Wiley) p15

[2] Young F W, Cathcart J V and Gwathmey A T 1956 *Acta Metall.* **4** 145

[3] Chang C A 1990 *J. Appl. Phys.* **67** 566

[4] Huang T C, Lim G, Parmigiani F and Kay E 1985 *J. Vac. Sci. Technol.* A **3** 2161

[5] Roy R A, Cuomo J J and Yee D S 1988 *J. Vac. Sci. Technol.* A **6** 1621

[6] Bai P, Yang G P and Lu T M 1990 *Appl. Phys. Lett.* **56** 198

[7] Burnett A F and Cech J M 1993 *J. Vac. Sci. Technol.* A **11** 2970

[8] Kim S P, Choi H M and Choi S K 1998 *Thin Solid Films* **322** 298

[9] Nye J F 1985 *Physical Properties of Crystals* (London: Oxford University Press)

[10] Zhang J M, Xu K W and Ji V 2001 *Appl. Surf. Sci.* **180** 1

[11] Ohmi T, Saito T, Shibata T and Nitta T 1988 *Appl. Phys. Lett.* **52** 2236

[12] Ohmi T, Saito T, Otsuki M, Shibata T and Nitta T 1991 *J. Electrochem. Soc.* **138** 1089

[13] Gangulee A 1972 *J. Appl. Phys.* **43** 867

[14] Li J, Mayer J W and Colgan E G 1991*J. Appl. Phys.* **70** 2820

[15] Zeng Y, Zou Y L and Alford Y L 1997 *Thin Solid Films* **307** 89

[16] Adamik M, Barna P B and Tomov I 2000 *Thin Solid Films* **359** 33

[17] Tracy D P and Knorr D B 1993 *J. Electronic Mater.* **22** 611

[18] Flinn P A 1991 *J. Mater. Res.* **6** 1498

[19] Knorr D B and Lu T M 1991 *Textures and Microstructures* **13** 155

[20] Junginger R and Elsner G 1988 *J. Electrochem. Soc.* **135** 2304

[21] Zhang J M and Xu K W 2003 *Acta Phys. Sin.* **52** 145 (in Chinese)

[22] Zhang J M and Xu K W 2002 *Acta Phys. Sin.* **51** 2562 (in Chinese)

[23] Zhang J M, Xu K W and Zhang M R 2003 *Acta Phys. Sin.* **52** 1207 (in Chinese)

[24] Wong C C, Smith H I and Thompson C V 1986 *Appl. Phys. Lett.* **48** 335

[25] Gangulee A and D'heurle F M 1972 *Thin Solid Films* **12** 399

[26] Longworth H P and Thompson C V 1991 *J. Appl. Phys.* **69** 3929

[27] Thompson C V and Smith H I 1984 *Appl. Phys. Lett.* **44** 603

[28] Kim H J and Thompson C V 1990 *J. Appl. Phys.* **67** 757

[29] Palmer J E, Thompson C V and Smith H I 1987 *J. Appl. Phys.* **62** 2492

[30] Lee D N 1999 *J. Mater. Sci.* **34** 2575

[31] Baskes M I 1987 *Phys. Rev. Lett.* **59** 2666

[32] Baskes M I, Nelson J S and Wright A F 1989 *Phys. Rev.* B **40** 6086

[33] Daw M S and Baskes M I 1983 *Phys. Rev. Lett.* **50** 1285

[34] Daw M S and Baskes M I 1984 *Phys. Rev.* **29** 6443

[35] Nϕrskov K K and Lang N D 1980 *Phys. Rev.* B **21** 2131

[36] Stott M J and Zaremba E 1980 *Phys. Rev.* B **22** 1564

[37] Foiles S M, Baskes M I and Daw M S 1986 *Phys. Rev.* B **33** 7983

[38] Adams J B, Foiles S M and Wolfer W G 1989 *J. Mater. Res.* **4** 102

[39] Daw M S and Foiles S M 1987 *Phys. Rev. Lett.* **59** 2756

[40] Dodson B W 1987 *Phys. Rev.* B **35** 880

[41] Foiles S M 1985 *Phys. Rev.* B **32** 7685

[42] Foiles S M and Daw M S 1987 *J. Mater. Res.* **2** 5

[43] Daw M S and Hatcher R D 1985 *Solid State Communications* **56** 697

[44] Foiles S M 1985 *Phys. Rev.* B **32** 3409

[45] Baskes M I 1992 *Phys. Rev.* B **46** 2727